ELSEVIER

Advances in Colloid and Interface Science 116 (2005) 255 – 261

ADVANCES IN COLLOID AND INTERFACE SCIENCE

www.elsevier.com/locate/cis

Differential approach to the study of integral characteristics in polymer films

P. Smertenko [a,*], L. Fenenko [a], L. Brehmer [b,1], S. Schrader [c,2]

[a] *Department of Optoelectronics, V. Lashkaryov Institute of Semiconductor Physics, NASU 45, prospekt Nauki, 03028, Kyiv, Ukraine*
[b] *Department of Condensed Matter Physics, Institute for Physics, Potsdam University, Am Neuen Palais 10, Haus 19, D-14469 Potsdam, Germany*
[c] *University of Applied Sciences Wildau Friedrich-Engels-Str. 63, D-15745 Wildau, Germany*

Available online 10 August 2005

Abstract

The differential approach is based on the determination of dimensionless differential slope, for instance, of current–voltage characteristics (IVC), $I=f(V)$. This slope (α) is given by formula $\alpha=\mathrm{d}(\lg I)/\mathrm{d}(\lg V)$. With such definition the ranges of constancy of the $\alpha(V)$ dependency correspond to the part of IVC characterized by the power behaviour ($I\sim V^{\alpha}$). The differential slope of $\alpha(V)$ dependency $\gamma=\mathrm{d}(\lg\alpha)/\mathrm{d}\lg V$ determines the exponent behaviour of curve ($I\sim\exp\{eV^{\gamma}/kT\}$). Processing by the differential approach of the investigated theoretical or experimental characteristics permits us to determine the peculiarity of charge flow mechanisms, temperature behaviour of conductivity, etc. The theoretical base and some applications of differential approach to the investigation of the current–voltage, temperature and degradation characteristics of the polyaniline and poly(*p*-phenilenevinilene) based structures have been shown.

PACS: 72.80.Le; 73.50.−h; 73.61.−r; 82.35.Lr
Keywords: Differential approach; Dimensionless differential slope; Charge flow mechanism; Current–voltage characteristic

Contents

1. Introduction . . . 255
2. Definition of the differential approach . . . 256
3. Accuracy of α(x) and γ(x) . . . 256
4. Main carrier transport and injection regimes . . . 256
5. Differential approach application . . . 257
   5.1. Current–voltage and temperature characteristics of emeraldine polyaniline based structure . . . 257
   5.2. Degradation of ITO–PPV–PPQ–Ca–Al structure characteristics . . . 259
6. Conclusion . . . 260
Acknowledgments . . . 260
References . . . 260

1. Introduction

Usually, the analysis of experimental characteristics, such as current–voltage characteristic (IVC), watt–current (WIC), capacitance–voltage (CVC), temperature (TC) ones etc., implies the determination of linear regions of curves in various plots, for example, $I=f(V^n)$, $\lg I=f(V^n)$, $V=f(C^n)$, and $V=f(T^n)$, where I is the current, V is the voltage, C is the

* Corresponding author. Tel.: +7 380 44 525 6477; fax: +7 380 44 525 8342.
E-mail addresses: smertenko@isp.kiev.ua (P. Smertenko) brehmer@rz.uni-potsdam.de (L. Brehmer), schrader@igw.tfh-wildau.de (S. Schrader).
[1] Tel.: +49 331 977 1503; fax: +49 331 977 1457/1083.
[2] Tel.: +49 3375 508 293; fax: +49 3375 508 884.

0001-8686/$ - see front matter © 2005 Elsevier B.V. All rights reserved.
doi:10.1016/j.cis.2005.05.005

capacitance, T is the absolute temperature, and n is the digit or the fraction [1,2]. This approach is convenient in the simple cases, when $n=1, 2, -2$, and so on. However, there are many difficulties in more complicated cases, when the experimental curves are described by combinations of the power and exponential approximations. In these cases the differential approach seems to be very useful for analysis. Such approach has been successfully applied for of IVC [3,4], TC [5,6] and WIC [7].

The general analytical expression for the combination of power and exponential functions can be written as:

$$y(x) = Ax^{\alpha 0}\exp[\gamma/\gamma(x/x_0)^{\gamma}], \quad (1)$$

where y is the function, x is the argument, A and x_0 are the constants, α and γ are the differential slope of function $y(x)$ in the log–log plot. The formula similar to (1) was used earlier [5] for the analysis of temperature characteristics.

The differential approach allows determining quantitatively the peculiarities of curves, such as minima and maxima, power and exponential regions. The main difference of the proposed approach from other differential methods (first and second derivatives) is the dimensionless nature of α and γ values that makes somewhat easier the comparison of objects with different properties.

In this work, the mathematical basis of differential approach is developed and some examples of its applications for charge flow mechanisms, temperature and degradation behaviour in polymer structures are given.

2. Definition of the differential approach

The differential approach to the analysis of theoretical and experimental data implies the determination of dimensionless value [8]

$$\alpha(x) = \frac{\mathrm{d}(lgy)}{\mathrm{d}(lgx)} = \left(\frac{x}{y}\right) \times \left(\frac{\mathrm{d}y}{\mathrm{d}x}\right). \quad (2)$$

For the finite increments of the argument and the function the expression (2) can be rewritten as:

$$\alpha\left(\frac{x_n + x_{n+1}}{2}\right) = \left(\frac{x_{n+1} + x_n}{x_{n+1} - x_n}\right) \times \left(\frac{y_{n+1} - y_n}{y_{n+1} + y_n}\right). \quad (3)$$

The equivalent to α in thermometry is the dimensionless sensitivity. For IVC the α value is the ratio of the static resistance $R=V/I$ to the differential resistance $\mathrm{d}V/\mathrm{d}I$, or the ratio of the differential conductivity $\mathrm{d}I/\mathrm{d}V$ to the conductivity $\sigma=I/V$.

Similar to Eqs. (2) and (3), the expressions for γ value can be determined as

$$\gamma(x) = \frac{\mathrm{d}(lg\alpha)}{\mathrm{d}(lgx)} = \left(\frac{x}{\alpha}\right) \times \left(\frac{\mathrm{d}\alpha}{\mathrm{d}x}\right). \quad (4)$$

$$\gamma\left(\frac{x_k + x_{k+1}}{2}\right) = \left(\frac{x_{k+1} + x_k}{x_{k+1} - x_k}\right) \times \left(\frac{\alpha_{k+1} - \alpha_k}{\alpha_{k+1} + \alpha_k}\right), \quad (5)$$

where $x_k = \dfrac{(x_n + x_{n+1})}{2}$.

The α and γ values characterise the power law dependence $y(x)=x^{\alpha}$, and the exponential law $y(x)=\exp(x^{\gamma})$, respectively. While processing the experimental dependencies $y(x)$ using Eq. (2) or (3) one can reveal the regions of $\alpha=$const. These are the regions where the $y(x)$ dependence is adequately approximated by a power law. Similarly, while processing experimental dependencies $y(x)$ using Eq. (4) or (5) one will find the regions of $\gamma=$const. These ones correspond to exponential behaviour of $y(x)$.

3. Accuracy of $\alpha(x)$ and $\gamma(x)$

It should be noted that the procedure of minimizing of the slope error has been developed [9] to enhance the accuracy of $\alpha(x)$ and $\gamma(x)$ determination. This procedure implies the x step variation during y measurement and provides the lowest error of $\alpha(x)$ and $\gamma(x)$ determination [9]. This error minimizing is due to the exception of systematic error caused by the transition from the infinitesimal increment of the argument and the function to the finite one under differentiation (see Eqs. (2), (3), (4) and (5)).

The top error value (Δ_{α}) for $\alpha(x)$ is achieved at argument step

$$(V/\delta V)_{\mathrm{opt}} = 2\left[\left(\Delta_y + \alpha\Delta_x\right)/\alpha|\alpha^2 - 1|\right]^{1/3}. \quad (6)$$

It is determined by the equations

$$\Delta_{\alpha} = 0.3\left[|\alpha^2 - 1|/\alpha\right]^{1/3}\left(\Delta_y + \alpha\Delta_x\right)^{2/3}, \quad (7)$$

where $(V/\delta V)_{\mathrm{opt}}$ is the optimised step of argument, $\Delta_{x,y}$ are the relative errors of argument and function determination, correspondingly [9].

Analogously we have for $\gamma(x)$

$$\Delta_{\gamma} = 0.3\left[|\gamma^2 - 1|/\gamma\right]^{1/3}(\Delta_{\alpha} + \gamma\Delta_x)^{2/3}. \quad (8)$$

4. Main carrier transport and injection regimes

The mechanisms of charge transport in polymer structures are still under investigation. As noted in [10], there are two extreme types of carrier motion in solids:

- highly delocalised plane wave in a broad carrier band with relatively large free path;
- hopping from site to site being scattering at virtually every step.

The temperature dependence of these types of motion is characterised by:

- wide band carrier mobility $\mu \gg 1$ cm^2 V^{-1} s^{-1} and $\mu \propto T^{-n}$, $n>1$;
- strong localization of carriers $\mu \ll 1$ cm^2 V^{-1} s^{-1} and $\mu \propto \exp(-E/kT)$, where E is the activation energy.

In such a definition, the differential approach to processing of experimental data can indeed recognise and discriminate the mechanisms of charge carrier transport. The values of alpha and gamma for some known mechanisms are summarised in Table 1 [10].

The symbols in the table denote the following values: μ is charge carrier mobility, T is absolute temperature, h is Plank constant, k is Boltzmann constant, ω is frequency, F is the electric field; a is appropriate lattice constant, E_b is the polaron binding energy; A is cross section of polymer molecule, C_L is elastic constant for longitudinal waves in polymer chain, Δ is deformation potential, m^* is the electron effective mass, E is the activation energy; W_h is the activation energy for charge carriers hopping, $\xi=\alpha^{-1}$ is a localization length, N_0 is density of states, v_{ph} is average phonon frequency, σ_0 is a low field conductivity, and μ_0 is mobility at room temperature and low field.

The proposed approach can be especially useful in the case of very fine effects, for example, for transport in 3D disordered system with small dipole moments when the spatial correlation relies on the octupole moment of transport molecules. Here, the correlation function is of such short range that it is difficult to distinguish it from that produced by van der Waals forces or traps [10].

Injection processes have been investigated intensively in 1960th–1980th [10–16]. There were developed the theoretical fundamentals of contact-injection phenomena, including appropriate boundary conditions, charge density and recombination rate.

Analysis of mechanisms of charge carriers injection from the contacts into a solid, including wide gap semiconductors, as well as analysis of this carriers recombination exhibit the essential variety of injected charge carriers behaviour and their influence on the IVC (see Table 2). The physical parameters which can be obtained from the IVC approximation for each injection regime are also in the Table 2. Application of such approach to the investigation of solar cell test structures was demonstrated in [17].

5. Differential approach application

5.1. Current–voltage and temperature characteristics of emeraldine polyaniline based structure

The IVC of investigated In–PANI–In structures and differential slopes of some of them are shown in Fig. 1 [18].

The IVC did not experience dramatic changes (Fig. 1a) and only the differential method allowed authors to underline the fine changing in behaviour of the curves (Figs. 1b and c). From Fig. 1b and c we can see a characteristic range with $\alpha=1.25$. Such α value cannot be explained by the bimolecular recombination (R) in the structure, when the minority (n) and majority (p) charge carriers concentrations

Table 1
Main approximations of carrier transport and corresponding temperature and voltage dependencies

Parameter value		Mobility and conductivity approximation	Regime peculiarities	Physical parameters
α	γ			
Temperature dependence				
−2.5	–	$\mu \propto T^{-2.5}$	Delocalised carriers in durene, band model with phonon scattering	
−1	−1	$\mu=(h\omega/kT)\exp(h\omega/kT)$	Polaron theory of Holstein, $T\leq h\omega/2\pi$	ω
−1	−1	$\mu \propto [(kT)/(eFa)\sinh[(eFa)/(2kT)\times\exp[-(eFa)^2/(8E_bkT)]]$	Theory of small polaron in antracene and naphthalene, mobility according Efros	E_b
−1/2	−1	$\mu=(2\pi ea^2/kTh)(\pi/2E_bkT)^{1/2}J^2\exp(-E_b/2kT)$	Hopping model for small polarons and narrow-phonon-band in the nondiabatic limit	E_b
1/2		$\mu=4A(2/\pi)^{1/2}[(C_Lh^2)/(\Delta^2m^{*3/2}(kT)^{1/2})]$	Mobility across the polymer molecule	
1	−1	$\mu=(ea^2\omega/6kT)\exp\{-W_h/kT\}$	Activated hopping of electrons	W_h
3/2		$\mu \propto T^{3/2}$	Scattering on acoustic phonons	
–	−1	$\mu \propto \exp(-E/kT)$	Hopping model	E
–	−1	$\mu=\mu_0\exp[-\Delta/kT]\exp\{\beta F^{1/2}[(1/kT)-(1/kT_0)]\}$	Mobility in disordered polymeric doped materials	T_0
1/2	−1/4	$\sigma=2(9\xi N_0/8\pi kT)^{1/2}v_{ph}\exp[-(T_0/T)^{1/4}]$; here $T_0=16/kN_0\xi$	Transport with variable range hopping	ξ
11–13	−1/4	$\sigma \propto T^n$; $\sigma \propto \sigma_0\exp\{-(T_0/T)^{1/4}\}$	Soliton transport	ξ
Field dependence				
	1/2	$\mu=\mu_0\exp[-\Delta/kT]\exp\{\beta F^{1/2}[(1/kT)-(1/kT_0)]\}$; here $\beta=1/kT$	Mobility in disordered polymeric doped materials	
	1/2	$\sigma=\sigma_0\exp(\beta F^{1/2}/kT)$; here $\beta=(e^3/\pi\varepsilon\varepsilon_0)^{1/2}$	Poole–Frenkel effect	
	3/4	$\mu \propto \exp[-(\sigma_q\beta)^2+(2^{3/2}/3^{1/4})(ea\beta F)^{3/4}(\sigma_q\beta)^{1/2}]$ here $\beta=1/k_BT$	Transport in 3D disordered system with small dipole moments	
	5/6	$\ln\mu \propto F^{5/6}$	Transport in 3D disordered system with small dipole moments when the spatial correlation relies on the octuple moment of transport molecules	

Table 2
Main approximations of $I-V$ characteristics and corresponding injection and recombination mechanisms

Value of α	$I-V$ characteristic approximation	Recombination and injection peculiarities	Physical parameters
1	2	3	4
$0<\alpha<1$ min	$j(V)=e\mu n_K \frac{V\exp\{\varepsilon e d_K V/\varepsilon_K kTL\}}{L(1+2\mu V/u_n D_K L)}$	Regime of constant field between contacts	n_K; S_K; d_K;
1	$j(V)=e\mu n_O V/L$	Ohm's law	n_0
1	$j(V)=e\mu n_K(V-V_K)/L$	Contact limited current	n_K; ρ_K/e
$1<\alpha<1.5$	$V(j)=[1-j/j_i]jL/\sigma$	Low injection	ρ_K/e
1.5	$j(V)=\frac{8}{9}e\sqrt{\frac{2\mu_n/\mu_p(\mu_n+\mu_p)}{\gamma}}\frac{V^{3/2}}{L^2}$	Double injection in semiconductor, bimolecular recombination of carriers	n_s; γ
2	$j(V)=\frac{9}{8}\frac{\varepsilon\mu V^2}{L^3}$	Monopolar injection in semiconductor or dielectric without traps	–
2	$j(V)=\frac{9}{8}\theta\frac{\varepsilon\mu V^2}{L^3}$	Monopolar injection in semiconductor or dielectric with traps	θ
2	$j(V)=\frac{3}{4}e\sqrt{\frac{\pi\varepsilon\mu_n\mu_p(\mu_n+\mu_p)}{\gamma}}\frac{V^2}{L^3}$	Double injection in ideal dielectric, bimolecular recombination of carriers	n_s; γ
2	$j(V)=\frac{9}{4}e\mu_n\mu_p\frac{(\gamma_n+\gamma_p)}{\gamma_n\gamma_p N_r}\Delta N\frac{V^2}{L^3}$	Double injection in ideal dielectric, monomolecular recombination of carriers	$\frac{\gamma_n\gamma_p}{\gamma_n+\gamma_p}N_r$
$\alpha>2$ max	–	Traps field limited (monopolar injection) or recombination limited (double injection)	$S(E)$; $R(E)$; N_r; E_r; $\tau_{n,p}$
3	$j(V)=\frac{125}{72\pi}e\mu_n\mu_p\tau\frac{V^3}{L^5}$	Double injection in ideal dielectric, monomolecular recombination of carriers	n_s; τ
4	$j(V)=\frac{21609}{131072\pi^2}\frac{eh^6}{(\gamma E_g)^3}\sqrt{\frac{\mu_n\mu_p(m_n+m_p)}{m_n m_p}}\times\frac{1}{\mu_n+\mu_p}\frac{V^4}{L^7}$	Super high double injection level	n_s; L_s; γ

are equal, another way, $R=\gamma np=\gamma p^2$, where γ is recombination coefficient [10,16]. Note, at low temperatures the $I\sim V^{5/4}$ region goes after Ohm's law whereas at room temperatures it dominates in all bias range. This evidences the promotion of the carriers injection with increase of temperature. Thus the injection behaviour entirely differs from that in a crystalline solid state [12].

The symbols in the table denote the following values: j, j_n; j_p are the full, electron and hole current densities, respectively; e is the electron charge ε, ε_K are the dielectric constants of the semiconductor and contact gap, respectively; μ_n, μ_p are the mobility of electrons and holes, respectively; E_g is the forbidden gap of the semiconductor; γ, γ_n, γ_p are the coefficients of zone–zone, electron and hole recombination, respectively; n_O, n_K, n_s are the ohmic, contact, and bulk current carriers concentrations, respectively; S_K is the surface recombination rate; d_K is the contact gap width; ρ_K/e is the near-contact charge density; L_s is the ambipolar diffusion length; τ and τ_p are the average life time of and electrons and holes; and θ is the sticking coefficient.

To clarify the transport mechanism in the investigated structures the temperature characteristics were measured (Fig. 2). Fig. 3 represents the differential slope of temperature characteristics under low and high biases.

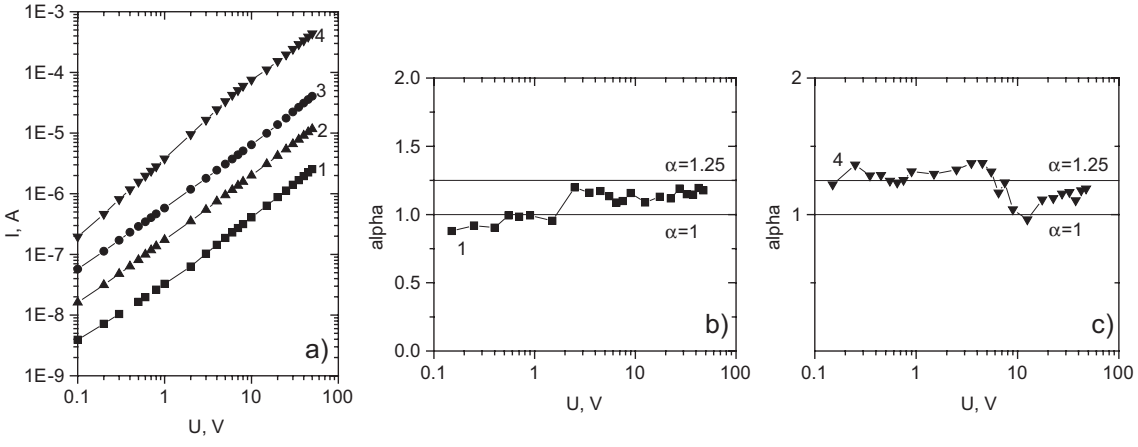

Fig. 1. $I-V$ characteristics of In–PANI–In structure at various temperatures: 1–153 K; 2–184 K; 3–240 K; 4–294 K (a) and differential slope of 1 (b) and 4 (c) curves.

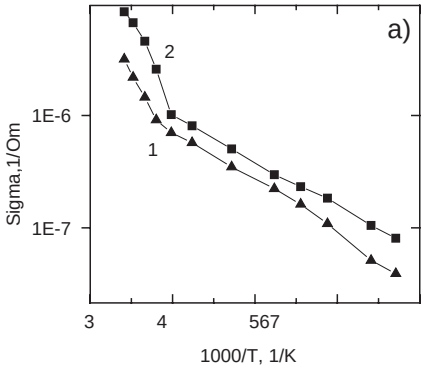

Fig. 2. Temperature characteristics of In–PANI–In structure at 0.1 V (1) and 50 V (2).

One can see that the temperature characteristics in the both cases of $V=0.1$ V and $V=50$ V (Figs. 2 and 3a, b) possess a constant slope in the range from 160 K to 250 K. This gives the activation energy of about 0.23 eV. Approximation of this range ($\sigma \sim \exp[-(1000/T)]$, line 3) cannot be changed with biases. In our opinion the results of Fig. 3 are more close to the case of intersoliton hopping [10], for which it is predicted the steady-state conductivity vs. temperature dependence in the form $\sigma \sim T^{\alpha}$, where α equals 11 to 13. In Fig. 3c we have $\alpha=11.2$. S. Kivelson noted [19] that temperature dependence of steady-state conductivity can be described in a good manner by both $\sigma \sim T^{\alpha}$ and $\sigma \sim \sigma_0 \exp[-(T_0/T)^{1/4}]$ formulas. Last approximation shows good correlation with the hopping model that supposes a changeable length between the states localized in the forbidden gap. Really, from Fig. 3a, b, c, and d one can see that the both approximations can describe experimental $\alpha(1/T)$ dependence.

5.2. Degradation of ITO–PPV–PPQ–Ca–Al structure characteristics

In Fig. 4 the degradation of the voltage drop of ITO/PPV/PPQ/Ca/Al structures is represented. Figs. 4a and b show the voltage drop of ITO/PPV/PPQ/Ca/Al structures in a usual and semilog plot, respectively. There are no regions of constancy on $\alpha(V)$ dependence (Fig. 4c) and, respectively, no the power dependencies. In spite of the noise on $\gamma(V)$ dependence, we found two regions with $\gamma \approx 0.5$ and $\gamma \approx 0.25$ (Fig. 4d). An accurate definition gave us two regions with corresponding approximations: $V=V_0\exp\{t_0/t^{0.38}\}$; where $V_0=6.146$; $t_0=0.01059$; (first region) and $V=V_0\exp\{t_0/t^{0.25}\}$; where $V_0=5.857$; $t_0=0.033$; (second region). These curves and their slope are presented in Fig. 4b and c, respectively. To represent the accuracy of approximations, the values the ratio between error (experimental function (F_{exp}) minus modelling one (F_{mod})) and experimental function for two regions are presented in Fig. 4e and f,

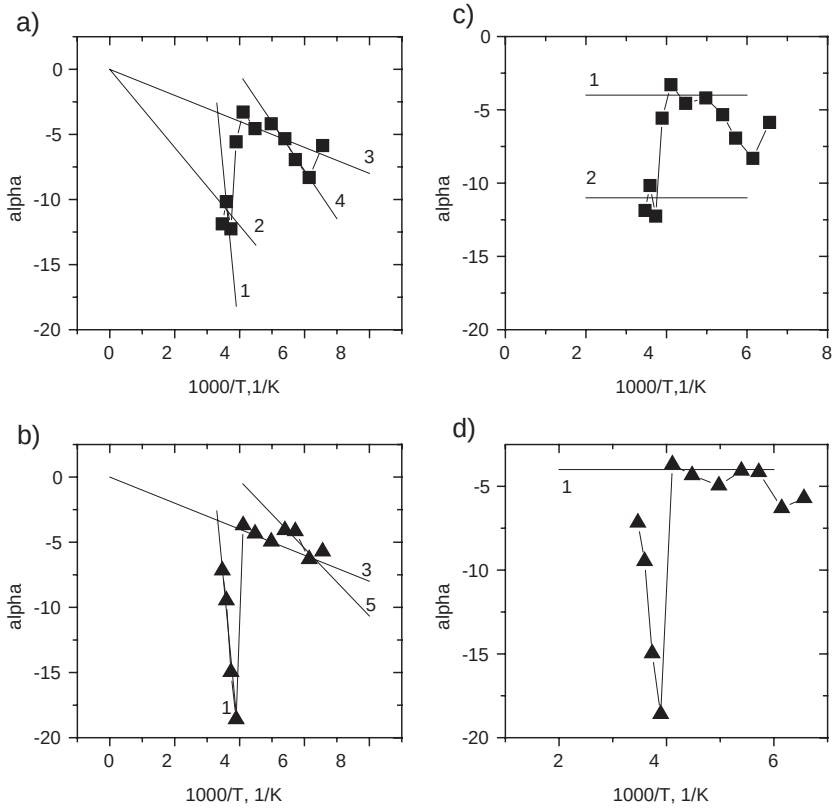

Fig. 3. Approximation of the differential slope $\alpha(1/T)$ of temperature characteristic for In–PANI–In structure at biases 0.1 V (a, c) and 50 V (b, d) in the form: for (a), (b): $\alpha(1/T)=-26(1000/T-3.2)$ (line 1); $\alpha(1/T)=-(3000/T)$ (line 2); $\alpha(1/T)=-(1000/T)$ (line 3); $\alpha(1/T)=-3.7(1000/T-3.9)$ (line 4); $\alpha(1/T)=-2.6(1000/T-3.9)$ (line 5) and for (c), (d): $\alpha(1/T)=-1000/T)^{-4}$ (line 1); $\alpha(1/T)=-(1000/T)^{-11}$ (line 2).

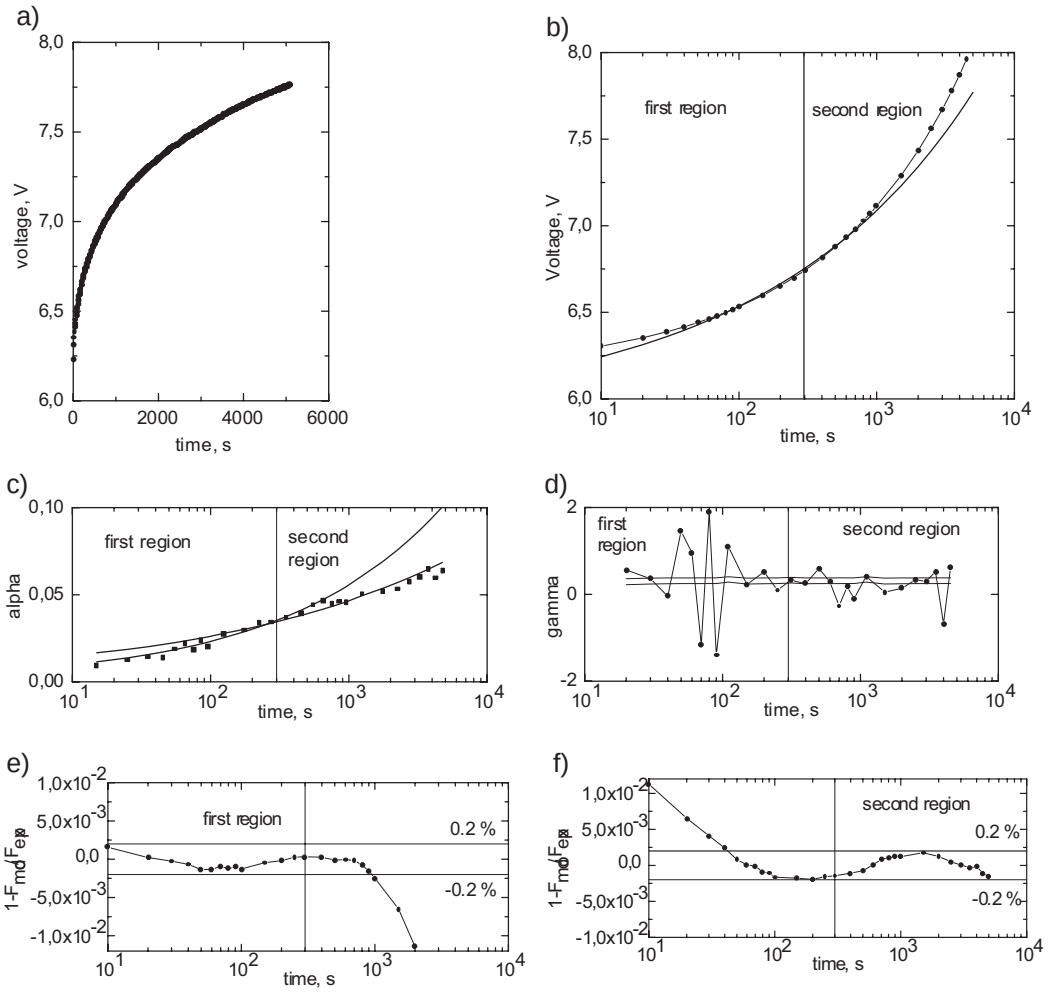

Fig. 4. a) degradation of the voltage drop of ITO/PPV/PPQ/Ca/Al structures in a usual plot; b) modeling of curve by the two approximations: $V=V_0\exp\{t_0/t^{0.38}\}$; where $V_0=6.146$; $t_0=0.01059$; (first region) and $V=V_0\exp\{t_0/t^{0.25}\}$; where $V_0=5.857$; $t_0=0.033$; (second region); c) $\alpha(V)$ dependence with corresponding approximations; d) $\gamma(V)$ dependence with corresponding approximations; e) error of degradation modeling in the first region (F_{mod} is calculated function, F_{exp} is experimental function); f) error of degradation modeling in the second region. Straight line at 300 s shows the intersection of two approximations. The range of accuracy ±0.2% is shown.

respectively. One can see that the accuracy is less than 0.2% in all investigated ranges (see Fig. 4e, f). The parameters of both approximations are close to one another and the modelling curves are overlapped in wide range. This demonstrates the possibility to distinguish fine effects of the curve behaviour.

6. Conclusion

The differential approach based on the determination of dimensionless differential slope of integral characteristics, $y=f(x)$, can be an effective tool for investigation the peculiarities of charge flow mechanisms and other processes in polymer films (temperature behaviour of conductivity, degradation behaviour, etc.). Such approach is capable for analysis and detecting of both analytical approximations and experimental data by detecting the special points: minima, maxima, inflection points and ranges corresponding to the power or exponential behaviours. The application of differential approach for modelling of characteristics provides high accuracy (better than ±0.1%) of curves description.

Some examples of usage of the differential approach show its high comprehension of analysis.

Acknowledgments

This work was supported by DAAD program in Germany.

References

[1] Sze SM. Physics of semiconductor devices. New York, Chichester, Brisbane, Toronto, Singapore: A Wiley-Interscience Publication, John Wiley & Sons; 1981.
[2] Smith RA. Semiconductors. UK: Cambridge University Press; 1982.

[3] Nespurek S, Sworakowski J. Phys Status Solidi, A Appl Res 1978;49:K149.
[4] Pfister JC. Phys Status Solidi, A Appl Res 1974;24:K15.
[5] Zabrodski AG, Zinov'eva KN. Zhurnal eksperimentalnoy i teoreticheskoy fiziki (Rus) 1984;84:727.
[6] Temperature Measurement and Control, Lake Shore, USA, 1997.
[7] Nelson DF. Phys Rev 1966;149:574–9.
[8] Svechnikov SV, Smertenko PS, Smirnov AV, Spychak IO. Differential technique of integral characteristics analysis. Ukrainski Fizicheski Jurnal (Rus) 1998;43:234–7.
[9] Gusev MYu, Zyuganov AN, Svechnikov SV, Smertenko PS. Optoelektronika i poluprovodnikovaja tekhnika (Rus) 1988;14:26.
[10] Pope M, Swenberg ChE. Electronic processes in organic crystals and polymerssecond edition. New York: Oxford University Press; 1999.
[11] Stockman F. Uber Strom – Spannung – Kennlinien "Ohmsher" Kontakte bei Halbleitern und Isolatoren. Halbleiterprobleme, Viervag, Braunschweig, vol. 6; 1961. p. 279–320.
[12] Lampert M, Mark P. Current injection in solids. New York: Academic Press; 1970.
[13] Baron R, Mayer JW. Double injection in semiconductors. Semiconductors and semimetals, vol. 6. New York: Academic Press; 1970. p. 201–313.
[14] Pellegrini B. Sol St Electon 1974;17:217.
[15] Roderick EH. Metal–semiconductor contacts. Oxford: Claredon Press; 1978.
[16] Zyuganov AN, Svechnikov SV. Contact-injection phenomena in semiconductors. Kyiv: Naukova dumka (Rus); 1981.
[17] Ciach R, Dotsenko YuP, Naumov VV, Shmyryeva AN, Smertenko PS. Injection technique for study of solar cells test structures. Sol Energy Mater Sol Cells 2003;76/4:613–24.
[18] Fenenko LI, Kuzma M, Pochekaylova LP, Smertenko PS, Sukach GA, Svechnikov SV. Phys Chem Solid State 2001;2:65–8.
[19] Kivelson S. Mol Cryst Liq Cryst 1981;77:65.